Research on Chemical Intermediates (2020) 46:2099–2108
https://doi.org/10.1007/s11164-020-04080-4

Structures and electronic and magnetic properties of the 3*d* transition metal-substituted TMC_5N_8 clusters

Zhi Li[1] · Zhen Zhao[2] · Zhong-suo Liu[1] · Hong-bin Wang[1] · Qi Wang[1]

Received: 5 November 2019 / Accepted: 6 January 2020 / Published online: 11 January 2020

Abstract

The structures and electronic and spin properties of the 3*d* TMC_5N_8 clusters have been calculated using the PBE functional. The results demonstrate that the Zn atom substituting significantly distorts the C_6N_8 clusters. TM atoms prefer to substitute the C atom which is farthest away from the biasing N atom. The TM substituting dramatically reduces the structural stability of the C_6N_8 clusters except for ScC_5N_8, TiC_5N_8 and VC_5N_8. As for the ground-state TMC_5N_8 clusters, the TM substituting improves the kinetic stability of the C_6N_8 clusters except for Ti, Cr and Cu. TM atoms in the TMC_5N_8 clusters loss certain amount of electrons. A few 4*s* orbital electrons of TM atoms transferred to the N atoms in the TMC_5N_8 clusters. The maximum spin values of the TM atoms occur at Mn and Ni for the TMC_5N_8 clusters.

Keywords C_3N_4 clusters · Density functional theory · Electronic properties · Magnetic properties

Introduction

Graphitic carbon nitride (g-C_3N_4) has been paid much attention because of its low cost, easy preparation, excellent biocompatibility, outstanding chemical and thermal stability, etc.[1, 2]. Nevertheless, the photocatalytic efficiency of g-C_3N_4 is restricted by its low light absorption efficiency, slow charge mobility and fast electron–hole recombination rate [3]. Doping is an effective way to organize the electronic features of semiconductors [1]. Experimentally, the 3*d* transition metal (TM) elements (Ti [4, 5], V [6], Cr [7], Mn [8], Fe [1, 8–17], Co [8, 13, 15, 18–20], Ni [21], Cu [8, 9, 15, 22, 23] and Zn [8, 16, 24, 25]) have been extensively explored over years

✉ Zhi Li
lizhi81723700@163.com

1 School of Materials and Metallurgy, University of Science and Technology Liaoning, Anshan 114051, People's Republic of China

2 School of Chemistry and Life Science, Anshan Normal University, Anshan 114007, People's Republic of China

[4]. Theoretically, Ghosh et al. [26] have calculated the structures and electronic and magnetic attributes of the 3*d* TM substituting for g-C_3N_4 sheet. However, precise identification of the available active sites of g-C_3N_4 has not been explored [27] because E. Kroke have revealed gh-C_3N_4 is more stable than gt-C_3N_4 by the density functional theory (DFT) [28]. In the current work, the primitive cell (C_6N_8) of the gh-C_3N_4 is abstract and then the 3*d* TM atom substituting the C atoms of the C_6N_8 clusters is considered. Ma et al. [29] have revealed that metal doping could reduce the energy gap of g-C_3N_4 by DFT calculations. If 3*d* TM substituted will reduce the energy gap of the C_6N_8 clusters? The TM atom substituting can modulate the electronic and magnetic properties of materials. It plays a crucial role in the diluted magnetic semiconductors [30]. So the structures, stability and electronic and spin properties of the TMC_5N_8 clusters are calculated by using DFT. It is very important to prepare the novel C_3N_4-based materials.

Computational details

The C_6N_8 clusters are abstract by the primitive cell of gh-C_3N_4 in Ref. [28]. And then, the TMC_5N_8 clusters are created by substituting a C atom for the C_6N_8 clusters by a TM atom. Hypothetical constructions of the TMC_5N_8 clusters must be optimized. The optimized process and properties calculations are performed by DFT which are embedded in the DMol^3 package. The Perdew–Burke–Ernzerhof (PBE) functional (including a semiempirical van der Waals (vdW) correction) within the generalized gradient approximation (GGA) is selected for the exchange–correlation [26, 31]. Due to the strong interaction between the TM atoms and the N atoms [32], Coulomb exclusion U must be considered [33]. To avoid missing the lowest-energy structures, symmetry unconstraints must be adopted [34, 35]. All electron relativistic treatments are selected due to the electron relativity effects of the TM atoms [36]. Spin polarization is chosen because certain TM atoms possess high spin values [35]. Double numerical plus polarization (DNP) is adopted [37]. Furthermore, the Mülliken population analysis is executed to get the electronic and spin characteristics of the TMC_5N_8 clusters [35].

In order to confirm whether the substituting can improve the structural stabilities of the TMC_5N_8 clusters, the average binding energy (E_b) of them was calculated [35]:

$$E_{b1} = [E(\mathrm{TM}) + 5E(\mathrm{C}) + 8E(\mathrm{N}) - E(\mathrm{TMC_5N_8})]/14 \quad (1)$$

where E(TM), E(C) and E(N) present the energy of the single TM, C and N atoms, respectively. $E(TMC_5N_8)$ is the total energy of the TMC_5N_8 clusters.

To determine the feasibility of the PBE functional considered, the calculated distance (6.840 Å) between two nitride pores is compared with the experimental result (6.81 Å) [38]. And the calculated lattice constant (7.138 Å) of gh-C_3N_4 agrees well with the computational values (7.13 Å [39] and 7.14 Å [40]) and the experimental result (7.13 Å [41]). Therefore, the PBE functional is adopted to analyze the TMC_5N_8 clusters.

Results and discussion

Structures

Optimized configurations of the TMC_5N_8 clusters are shown in Fig. 1. The C atoms are described as gray balls, the N atoms are described as blue balls, and the TM atoms are described as other balls. As for the TMC_5N_8 clusters, the planar structure of the C_6N_8 clusters is distorted to different degrees. It is derived that the TM atoms can increase the coupling between the unoccupied molecular orbitals (UMOs) with occupied molecular orbitals (OMOs), which leads to pseudo-Jahn–Teller (PJT) distortion and the characteristic buckling [42]. 3*d* atoms prefer to substitute the C atom which is farthest away from the biasing N atom. However, TM atoms substitute the C atom which approaches the biasing N atom of the C_6N_8 clusters. The isomers (c) are the most unstable structures. All the structures of the TMC_5N_8 clusters inherit those of the C_6N_8 clusters except for the ZnC_5N_8 clusters. The radius of the TM atoms are larger than that of the substituted C atoms. It results in the C_1 symmetry. As for significant distortion of the ZnC_5N_8 clusters, it derives from the *d*-*p* repulsion interaction between the 3*d* orbital electrons of the Zn atom and the 2*p* orbital electrons of the N atoms [24]. Wang et al. [2] have pointed out the pore diameter of Zn doped C_3N_4 has increased compared with g-C_3N_4 by the BET analysis. It attributes to the aggregate effect of Zn-N bond [2]. Our calculated TMC_5N_8 clusters indeed undergo an obvious deformation.

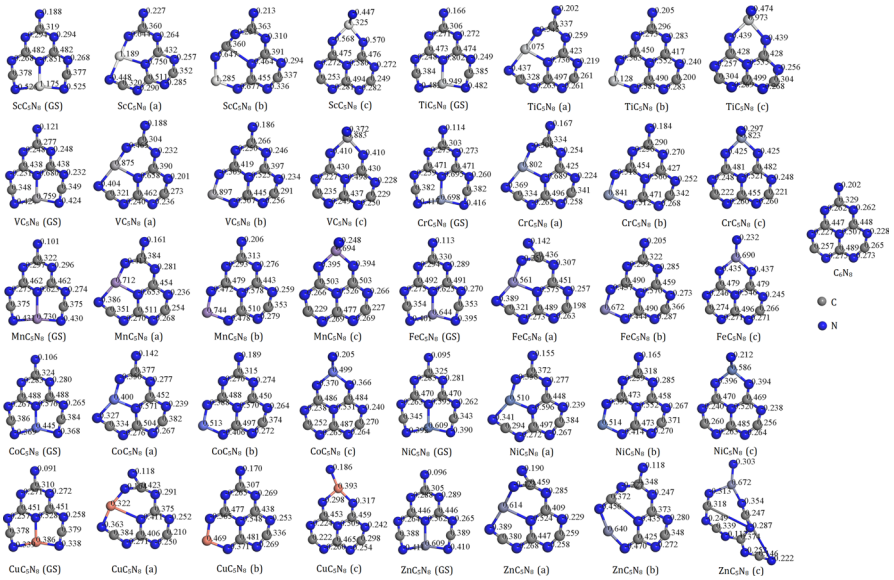

Fig. 1 Structures and charges of the C_6N_8 and TMC_5N_8 clusters. (Color figure online)

Stability

The average binding energies E_b of the TMC_5N_8 clusters are plotted in Fig. 2. The chemical element symbols which are corresponding to the abscissa are shown in Fig. 2. Due to the more negative binding energy, the more stable the structure, compare the average binding energy E_b of the C_6N_8 clusters, it can be found that all the TM substituting reduces the structural stability of the C_6N_8 clusters except for ScC_5N_8, TiC_5N_8 and VC_5N_8. It means that the TM atoms prefer to segregate and then aggregate TM clusters [26]. From Fig. 2, it can also be found that the ground-state TMC_5N_8 clusters have slightly more structural stability than the other isomers. Oh et al. [15] have pointed out C_3N_4 is thermally stable up to 500 °C by the thermogravimetric analysis. However, once the temperature is further increased, the binding will weaken because of thermal fluctuation [43]. As for the TMC_5N_8 clusters,

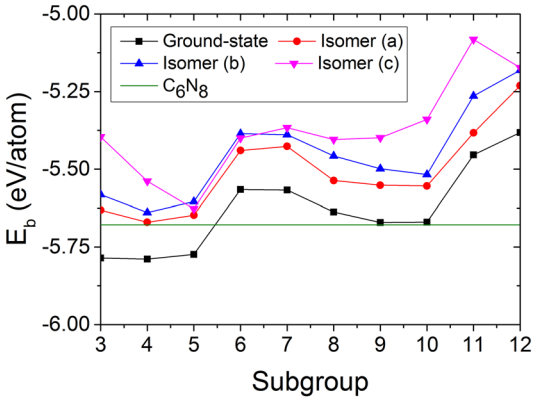

Fig. 2 Average binding energies of the TMC_5N_8 clusters

	3	4	5	6	7	8	9	10	11	12
3*d*	Sc	Ti	V	Cr	Mn	Fe	Co	Ni	Cu	Zn

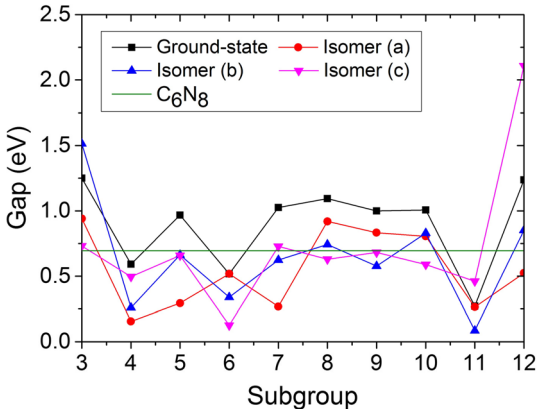

Fig. 3 The HOMO–LUMO gaps of the TMC_5N_8 clusters

the abnormal stretching in the C_6N_8 clusters due to the TM substituting will cause the fracture of the C-N bond at a lower temperature. TM atoms will promote the transition of the quasi-planar structures into 3D-cluster-like structures [44]. Xiong et al. [45] have found the nano-structural transformation from graphitic-like CN_x to fullerene-like β-C_3N_4 with the increase in the temperature by TEM observation and blue-shift photoluminescence peaks. However, the cross-link effect of Zn between inter-layers obstructs the exfoliation of g-C_3N_4 [2].

The energy gaps between the highest occupied molecular orbital (HOMO) states and the lowest unoccupied molecular orbital (LUMO) states of the TMC_5N_8 clusters which can analyze the chemical reaction process are shown in Fig. 3. The calculated HOMO–LUMO gap (0.694 eV) of the C_6N_8 clusters is much narrower than the experimental value (2.7 eV) of C_3N_4. Zhu et al. [39] have also revealed that the band gap (1.24 eV) in monolayer CN is smaller than the experimental value above. It is not only the well-known shortcomings (the lower exchange correlation between electrons) of the GGA functional, but also the difference between the systems. The larger HOMO-LUMO gap, the higher kinetic stability. Compare the energy gap of the ground-state TMC_5N_8 clusters, it indicates that the TM substituting can improve the kinetic stability of the C_6N_8 cluster except for Ti, Cr and Cu. Ding et al. [4] have found a slightly red shift from 465 to 467 nm due to Ti-doped the pristine C_3N_4 by the photoluminescence emission spectrum, which confirm to the narrowed band-gap by Ti doping. As for the isomers (a), only the Sc, Fe, Co and Ni substituting can improve the kinetic stability of the C_6N_8 clusters. Zhu et al. [39] have pointed out the 3*d* electrons of the doped Co have an excellent contribution to the reduction in the band gap of Co-CN by the characterization and density functional theory (DFT). As for the isomers (b), only the Sc, Fe, Ni and Zn substituting will improve the kinetic stability of the C_6N_8 clusters. Oh et al. [15] have observed that Fe has a relatively stronger coordination interaction with g-C_3N_4 than Co and Cu by the XRD peak shifting. As for the isomers (c), only the Sc, Mn and Zn substituting will increase the kinetic stability of the C_6N_8 clusters. It is derived that these TM atoms are quite appropriate for the "nitrogen pots" characteristic which possesses six lone-pair electrons [1]. From another perspective, the Ti, Cr and Cu substituting significantly improves the kinetic activity of the C_6N_8 clusters. As for the isomers (a), only the Ti, Mn and Cu substituting improves the kinetic activity of the C_6N_8 clusters. As for the isomers (b), only the Ti, Cr, Co and Cu substituting improves the kinetic activity of the C_6N_8 clusters. As for the isomers (c), only the Ti, Cr, Fe and Cu substituting improves the kinetic activity of the C_6N_8 clusters. It is because of the hybridization between *d* orbitals of the TM atoms and *p* orbitals of the C_6N_8 clusters [26]. Further, the TM atoms lead to the strengthening of the vibronic coupling in the OMO-UMO pairs. The vibrational instability leads to the planar C_6N_8 clusters transfer to the puckered TMC_5N_8 structures [42]. The TMC_5N_8 clusters which possess metal-like dense electronic density of states will lead to non-adiabatic instability for the C_3N_4 [46].

To further understand the effect of the TM atom substituting for the C_6N_8 clusters, the HOMO and LUMO states of the ground-state TMC_5N_8 clusters are demonstrated in Table 1. The blue regions prefer to trap electrons, and the yellow regions prefer to release electrons. It is shown that for the majority of

Table 1 The HOMO and LUMO orbitals of the ground-state TMC_5N_8 clusters

Cluster	HOMO	LUMO
ScC_5N_8	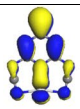	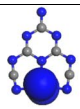
TiC_5N_8	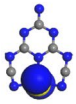	
VC_5N_8		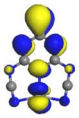
CrC_5N_8		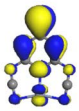
MnC_5N_8		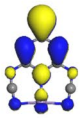
FeC_5N_8		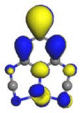
CoC_5N_8		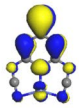
NiC_5N_8	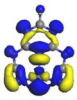	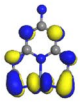
CuC_5N_8		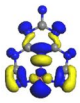
ZnC_5N_8		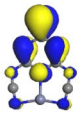

the TMC_5N_8 clusters, the HOMO and LUMO states have evident hybridization between the 3*d* orbital electrons of the TM atoms and the 2*p* orbital electrons of the N atoms, while for the ZnC_5N_8 clusters, the hybridization effect is rare because the Zn atoms are the $3d^{10}$ systems which contain all paired *d* orbital electrons [26].

Electronic properties

The net charges of the TM atoms for the TMC_5N_8 clusters are displayed in Fig. 4; it can be found that for the ground-state TMC_5N_8 clusters, the TM atoms loss a small amount of electrons within the scope of 0.375 |e| and 0.931 |e| except for Sc loss 1.150 |e|. Charge transfer of Co and CN molecules has been confirmed by Raman enhancement factors [39]. Zhu et al. [39] have also found that the three N atoms gain 1.03|e| on average, while Co atom loses 0.94|e| through the Bader analysis. As for the differences in the net charges of TM atoms for the TMC_5N_8 isomers in Fig. 4 and the Mülliken charges of the C and N atoms for the TMC_5N_8 clusters in Fig. 1, it is derived that the atomic coordination number [47] and atomic arrangements [48] of the TMC_5N_8 clusters affect the electron transferred at a certain level.

The natural electron configurations of the ground-states TMC_5N_8 clusters are included in Table 2. Comparing the natural electron configurations (Sc: $3d^14s^2$, Ti: $3d^24s^2$, V: $3d^34s^2$, Cr: $3d^54s^1$, Mn: $3d^54s^2$, Fe: $3d^64s^2$, Co: $3d^74s^2$, Ni: $3d^84s^2$ Cu: $3d^{10}4s^1$ and Zn: $3d^{10}4s^2$) of the isolated TM atoms with those of the TM atoms for the TMC_5N_8 clusters in Table 2, it can be found that the 3*d* and 4*p* orbitals of the TM atoms acquire a few electrons. In contrary, the 4*s* orbital of the TM atoms loses a small amount of electrons. It further confirms the hybridization mechanism of the *sp* orbital electrons of the TM atoms in the TMC_5N_8 clusters. Zhu et al. [39] have found that the 3*d* electrons of the Co atom and 2*p* electrons from the nearest neighboring N are hybrid by the XPS analysis.

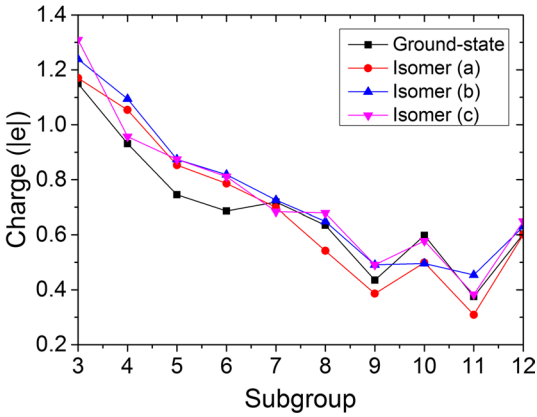

Fig. 4 The net charges of the TM atoms for the TMC_5N_8 clusters

Table 2 Natural electron configurations of the TM atoms for the ground-state TMC_5N_8 clusters

Cluster	Atom	Natural electron configuration
ScC_5N_8	Sc	[core]3*d*(1.402)4*s*(0.190)4*p*(0.266)
TiC_5N_8	Ti	[core]3*d*(2.463)4*s*(0.315)4*p*(0.302)
VC_5N_8	V	[core]3*d*(3.565)4*s*(0.328)4*p*(0.355)
CrC_5N_8	Cr	[core]3*d*(4.574)4*s*(0.356)4*p*(0.406)
MnC_5N_8	Mn	[core]3*d*(5.431)4*s*(0.423)4*p*(0.418)
FeC_5N_8	Fe	[core]3*d*(6.581)4*s*(0.354)4*p*(0.421)
CoC_5N_8	Co	[core]3*d*(7.635)4*s*(0.443)4*p*(0.480)
NiC_5N_8	Ni	[core]3*d*(8.525)4*s*(0.447)4*p*(0.424)
CuC_5N_8	Cu	[core]3*d*(9.613)4*s*(0.507)4*p*(0.512)
ZnC_5N_8	Zn	[core]3*d*(10.102)4*s*(0.631)4*p*(0.663)

Magnetic properties

Incorporation of spin-polarized 3*d* TM atoms in the g-C_3N_4 systems is an effective method to adjust spin moment [26]. The spin values of TM atoms in the TMC_5N_8 clusters are shown in Fig. 5. It can be found that for the TM atoms in the TMC_5N_8 clusters, all the spin densities are lower than those for isolated TM atoms in Ref. [36], and it is mainly derived from the origin of different kinds of magnetic couplings in these planar sheets can be understood by considering the spatial arrangement of interacting magnetic orbitals [26]. And the spin directions of the N atoms are opposite to that of the TM atoms [26]. As for the ground-state TMC_5N_8 clusters, the maximum spin values of the TM atoms occurred in Mn and Ni. It is derived that the 3*d* orbitals of Mn display strong spin exchange splitting ε_d [49], while for Cu and Zn atoms they display the non-magnetic states due to the all paired *d* orbital structures [26]. As for $Spin_{Mn} > Spin_{Fe} > Spin_{Ni} > Spin_{Co}$, it is derived that the minority spin gaps E_{min} decreased as the numbers of 3*d* electrons increased [49]. As for the discrete spin values of these TMC_5N_8 isomers, it derives from the spatial

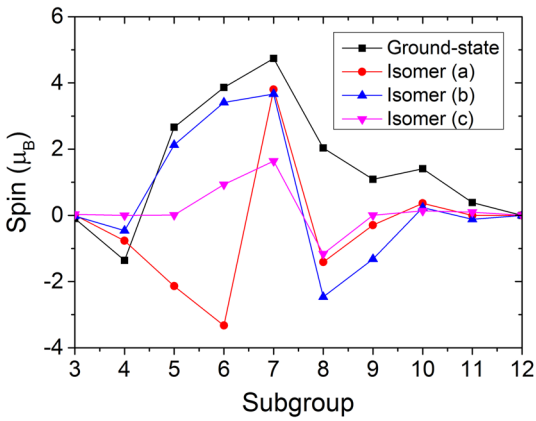

Fig. 5 The spins of the TM atoms for the TMC_5N_8 clusters

arrangements of interacting magnetic orbitals [26]. D. Ghosh et al. [26] have also pointed out that the V, Cr and Fe atoms interact with the g-C_3N_4, which exhibits ferromagnetic states.

Conclusions

In summary, the structures and electronic and spin properties of the 3*d* TMC_5N_8 clusters have been calculated by using first-principles. The results reveal that the Zn atoms can significantly distort the C_6N_8 clusters. 3*d* TM atoms prefer to substitute the C atom which is farthest away from the biasing N atom except for ScC_5N_8, TiC_5N_8 and VC_5N_8 by the average binding energy. The TM substituting significantly reduces the structural stability of the C_6N_8 clusters by the average binding energy. As for the ground-state TMC_5N_8 clusters, the TM substituting improves the kinetic stability of the C_6N_8 clusters except for Ti, Cr and Cu by the HOMO–LUMO gaps. From the net-charge distribution of the TMC_5N_8 clusters, it can be found that the TM atoms loss a certain amount of electrons and a few 4*s* orbital electrons of TM atoms transferred to the N atoms. The maximum spin values of the TM atoms occur at Mn and Ni for the TMC_5N_8 clusters by the Mülliken population analysis.

Acknowledgements We gratefully acknowledge the financial support from the Key Fund Project of the National Science Foundation, People's Republic of China (Grant No. 51634004), the National Natural Science Foundation, People's Republic of China (Grant Nos. 51704149 and 51874172), the Doctoral Scientific Research Foundation of Liaoning Province (Grant No. 20180551213), Key Laboratory of Chemical Metallurgy Engineering Liaoning Province, University of Science and Technology LiaoNing (Grant No. USTLKFSY201711) and the Fund Project of University of Science and Technology Liaoning (Grant No. 2017YY02).

References

1. J. Gao, Y. Wang, S. Zhou, W. Lin, Y. Kong, ChemCatChem. **9**, 1708 (2017)
2. Z.T. Wang, J.L. Xu, H. Zhou, X. Zhang, Rare Metal **38**, 459 (2019)
3. C. Sun, H. Zhang, H. Liu, X. Zheng, W. Zou, L. Dong, L. Qi, Appl. Catal. B Environ. **235**, 66 (2018)
4. R. Zhang, S. Niu, X. Zhang, Z. Jiang, J. Zheng, C. Guo, Appl. Surf. Sci. **489**, 427 (2019)
5. Y. Wang, Y. Wang, Y. Chen, C. Yin, Y. Zuo, L.-F. Cui, Mater. Lett. **139**, 70 (2015)
6. G.D. Ding, W.T. Wang, T. Jiang, B.X. Han, H.L. Fan, G.Y. Yang, Chemcatchem. **5**, 192 (2013)
7. Y. Zhang, Q. Zhang, Q. Shi, Z. Cai, Z. Yang, Sep. Purif. Technol. **142**, 251 (2015)
8. Z. Ding, X. Chen, M. Antonietti, X. Wang, Chemsuschem **4**, 274 (2011)
9. Z. Li, C. Kong, G. Lu, J. Phys. Chem. C. **120**, 56 (2016)
10. P.F. Zhang, Y.T. Gong, H.R. Li, Z.R. Chen, Y. Wang, RSC Adv. **3**, 5121 (2013)
11. Q. Liu, T. Chen, Y. Guo, Z. Zhang, X. Fang, Appl. Catal. B Environ. **205**, 173 (2017)
12. J. Ma, Q. Yang, Y. Wen, W. Liu, Appl. Catal. B: Environ. **201**, 232 (2017)
13. X. Chen, J. Zhang, X. Fu, M. Antonietti, X. Wang, J. Am. Chem. Soc. **131**, 11658 (2009)
14. S. Tonda, S. Kumar, S. Kandula, V. Shanker, J. Mater. Chem. A. **2**, 6772 (2014)
15. W. Oh, V.W.C. Chang, Z. Hu, R. Goei, T. Lim, Chem. Eng. J. **323**, 260 (2017)
16. X.C. Wang, X.F. Chen, A. Thomas, X.Z. Fu, M. Antonietti, Adv. Mater. **21**, 1609 (2009)
17. H.A. Bicalho, J.L. Lopez, I. Binatti, P.F.R. Batista, J.D. Ardisson, R.R. Resende, E. Lorencon, Mol. Catal. **435**, 156 (2017)
18. Q. Liu, J.Y. Zhang, Langmuir **29**, 3821 (2013)

19. B. Sun, H. Li, H. Yu, D. Qian, M. Chen, Carbon **117**, 1 (2017)
20. L. Deng, M. Zhu, RSC Adv. **6**, 25670 (2016)
21. L. Kong, Y. Dong, P. Jiang, G. Wang, H. Zhang, N. Zhao, J. Mater. Chem. A. **4**, 9998 (2016)
22. B. Tahir, M. Tahir, N.A.S. Amin, Appl. Surf. Sci. **419**, 875 (2017)
23. M. Ji, J. Huang, K. Zhang, D. He, S. Chang, D. Luo, E. Zhang, M. Xu, J. Liu, J. Zhang, J. Xu, J. Wang, C. Zhu, Inorg. Chem. Front. **5**, 2420 (2018)
24. B. Yue, Q. Li, H. Iwai, T. Kako, J. Ye, Sci. Technol. Adv. Mater. **12**, 034401 (2011)
25. H. Sudrajat, S. Hartuti, Optik. **181**, 1057 (2019)
26. D. Ghosh, G. Periyasamy, B. Pandey, S.K. Pati, J. Mater. Chem. **2**, 7943 (2014)
27. S. Sarkar, S.S. Sumukh, K. Roy, N. Kamboj, T. Purkait, M. Das, R. Sundar Dey, J. Colloid Interf. Sci. **558**, 182 (2019)
28. E. Kroke, Angew. Chem. Int. Edit. **53**, 11134 (2014)
29. X. Ma, Y. Lv, J. Xu, Y. Liu, R. Zhang, Y. Zhu, J. Phys. Chem. C. **116**, 23485 (2012)
30. P. Wu, G. Cao, F. Tang, M. Huang, Comp. Mater. Sci. **86**, 180 (2014)
31. T. Wang, G. Yu, J. Liu, X. Huang, W. Chen, Phys. Chem. Chem. Phys. **21**, 1773 (2019)
32. Y. Yang, C. Yin, K. Li, H. Tang, Y. Wang, Z. Wu, J. Electrochem. Soc. **166**, F755 (2019)
33. S.A. Khandy, D.C. Gupta, RSC Adv. **6**, 48009 (2016)
34. Z. Zhao, Z. Li, Q. Wang, T. Shi, Mater. Chem. Phys. **240**, 122220 (2020)
35. Z. Zhao, Z. Li, Mod. Phys. Lett. B. **33**, 1950459 (2019)
36. Z. Zhao, Z. Li, Q. Wang, Chem. Phys. Lett. (2020)
37. B. Delley, J. Chem. Phys. **113**, 7756 (2000)
38. X. Wang, K. Maeda, A. Thomas, K. Takanabe, G. Xin, J.M. Carlsson, K. Domen, M. Antonietti, Nat. Mater. **8**, 76 (2009)
39. Z. Zhu, X. Tang, T. Wang, W. Fan, Z. Liu, C. Li, P. Huo, Y. Yan, Appl. Catal. B Environ. **241**, 319 (2018)
40. J. Cui, S. Liang, X. Wang, J. Zhang, J. Mater. Chem. Phys. **161**, 194 (2015)
41. P. Niu, L. Zhang, G. Liu, Adv. Funct. Mater. **22**, 4763 (2012)
42. D. Jose, A. Datta, J. Chem. Phys. C. **116**, 24639 (2012)
43. B. Saha, A. Datta, J. Phys. Chem. C. **122**, 19204 (2018)
44. T. Teshome, A. Datta, Acs Appl. Mater. Inter. **9**, 34213 (2017)
45. Z.-W. Xiong, L.-H. Cao, J. Alloy. Compd. **775**, 100 (2019)
46. S.M. Pratik, C. Chowdhury, R. Bhattacharjee, S. Jahiruddin, A. Datta, Chem. Phys. **460**, 101 (2015)
47. J.M. Recio, R. Pandey, A. Ayuela, A.B. Kunz, J. Chem. Phys. **98**, 4783 (1993)
48. G. Ge, Q. Jing, Z. Yang, Y. Luo, Chin. Phys. Lett. **26**, 083101 (2009)
49. L.J. Shi, Phys. Lett. A. **374**, 1292 (2010)